August 27-31, 2023
FLORENCE - ITALY
ICWE 16
16th International Conference on Wind Engineering

Aeroelastic modelling of solar trackers

Juan Zaracho [1], John Ginger [1], Korah Parackal [1], David Henderson [1]

[1]*Cyclone Testing Station, James Cook University, Townsville, Australia.*
juanignacio.zaracho@jcu.edu.au

SUMMARY:
Ground mounted "solar trackers" that rotate about a torque tube experience dynamic effects due to wind action that can influence their structural stability eventually causing failure. This study will investigate the fluctuating wind loads on solar trackers, determine their dynamic response such as vortex excitation and torsional galloping and study the interaction of multiple arrays in a solar farm. A series of aeroelastic models are built considering typical material and structural properties of solar trackers. These models will be tested in the wind tunnel where torque, rotational displacement and wind pressure will be measured.

Keywords: Solar tracker, aeroelastic model, wind load, dynamic effects

1. INTRODUCTION

Solar trackers systems (STS) comprise solar panel modules attached to frames that are fixed on to a torque tube that allows the system to rotate and orient towards the sun, thus increasing energy output up to 30% compared to fixed solar panel arrays. Slender components of STS experience dynamic effects due to wind action. These dynamic effects can eventually cause structural failure and hence must be analysed to enable satisfactory structural design methods. A study on torsional galloping conducted by Martínez-García et al (2021) demonstrated how the onset of torsional galloping is influenced by the inertia of the solar panels and the aspect ratio of the array considering the effect of the torque tube stiffness. Only one isolated structure was considered, which makes them equivalent to the first-row trackers of a solar farm. Valentín et al (2022) carried out a failure investigation of a STS farm due to torsional galloping. The structure was analysed in the field and a numerical model of the structure was used to identify natural frequencies as well as maximum stresses in the components of the system, confirming that the cause of the failure was torsional galloping occurring for high-speed winds and for a tilt angle of 0°.

2. AERODYNAMIC FORCES AND EFFECTS

2.1 Torsional Galloping

Torsional galloping is a form of single degree of freedom aerodynamic instability, which can occur for long bodies with certain cross-sections. The moment acting on the structure generates a twist on the torque tube, changing the initial position of the plate and changing the tilt angle α, so that $\alpha = -b\dot{\gamma}/2U$. Here, b is the chord length or breadth of the solar trackers, $\dot{\gamma}$ the angular velocity

of the system and U is the wind speed. The onset of torsional galloping on a structure is linked to a specific critical wind speed U_{cr} and is defined by Blevins (1990):

$$\frac{U_{cr}}{n_\gamma b} = -\frac{8J_0(2\pi\zeta)}{\rho b^4} \Big/ \frac{\partial C_M}{\partial \alpha} \quad (1)$$

Where, n_γ is the torsional vibration frequency, J_0 the polar moment of inertia, ζ is the critical damping ratio of the structure and C_M is a moment coefficient. The condition under which galloping would arise is defined by $\partial C_M/\partial\alpha < 0$.

2.2 Vortex-induced vibrations

These vibrations occur when shedding frequency matches the natural frequency of the structure. Chen and Fang (1996) measured the frequencies of vortex shedding from flat plates with beveled sharp edges at tilt angles α, from 0° to 90°, and a range of Re. They found that St is about 0.16 for typical α. This is important to consider as it allows frequencies of vortex shedding for different wind speeds to be determined. These can then be compared against natural frequencies of different types of STS to evaluate vortex-induced vibrations in the structure.

3. WIND TUNNEL STUDY

3.1 Rigid model test

This study was carried out in the 2.5m wide × 2m high × 22m long Boundary Layer Wind Tunnel at the Cyclone Testing Station, James Cook University. The approach Atmospheric Boundary Layer was simulated at a length scale L_r = 1/20. A basic 2.5m x 5m full-scale module consisting of sixteen (i.e. 8×2) 1.2m × 0.625m solar panels were built and combined to give a six-module configuration. Modules were constructed at a length scale of 1/20. Tests were carried out for typical tilt angles α and for different wind directions θ. Time ratio is given by $T_r = L_r/U_r = \left(\frac{1}{20}\right)/\left(\frac{1}{3}\right) = \frac{3}{20}$. Hence, $T_m = 0.15 \times 10\ min \times 60\ s = 90\ s$. Top and bottom surface pressures on each model were measured simultaneously to give net (i.e. (top-bottom)) pressure fluctuations. These fluctuating pressures were sampled at 100 Hz, for 90 sec (~ 10 mins in full scale), and the pressure coefficients $C_p(t) = p(t)/\left(\frac{1}{2}\rho\overline{U_h}^2\right)$ recorded. Results are shown in Figure 1.

	0.46	0.29	0.32	0.34	0.31	0.41	0.30	0.35	0.32	0.42	0.30
0.39	0.67	0.57	0.61	0.62	0.74	0.62	0.63	0.63	0.75	0.62	0.64
0.47	0.89	0.85	0.85	0.78	0.92	0.94	0.93	0.79	0.93	0.95	0.93
0.76	1.07	1.01	1.05	1.00	1.12	1.00	1.16	1.01	1.13	1.01	1.17
0.89	1.09	1.24	1.27	1.21	1.57	1.27	1.36	1.22	1.58	1.28	1.37
1.24	1.36	1.57	1.70	1.53	1.51	1.75	1.53	1.54	1.52	1.76	1.54
1.86	1.46	2.28	2.22	2.32	2.35	2.11	2.20	2.34	2.37	2.13	2.22
2.38	2.89	2.87	2.88	2.88	2.84		2.86	2.90	2.87		2.89
-2.48		-2.92		-2.84		-2.19		-2.87		-2.20	

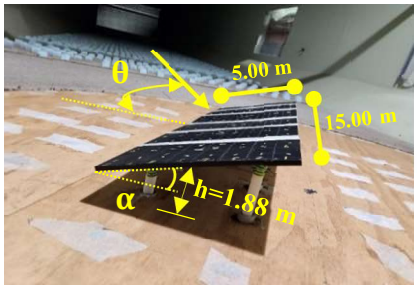

Figure 1. $\overline{C_p}$ and $\overline{C_M}$ on solar panel modules, α = 20° and θ = 0° (left). Six-module array in wind tunnel (right).

Results are consistent with those obtained by Ginger et al (2019) and others. The leading edge of the array develops high pressure which drops towards the downstream. Moment coefficients were calculated by $\overline{C_M} = \sum_{i=1}^{16} C_{pn_{b_i}} \cdot b_i/b$, where b_i is the distance from the axis at mid-height to the location of the pressure tap on the panel. In Figure 1, the mean torque tends to be similar on all modules of the array, being slightly smaller on the laterals. The direction of the torque on each panel is given by the pressure distribution, which resultant located nearby the leading edge, generates a counterclockwise turn.

3.2 Aeroelastic modelling

Rigid model tests can be carried out to obtain wind loading on structures, but aeroelastic models are required to evaluate the effects of aerodynamic forces. Aeroelastic modelling requires similarity of a series of non-dimensional parameters, such as: $St = nb/\bar{U}_z$; $Re = \rho\bar{U}_z b/\mu$; Density ratio = ρ_s/ρ; Froude number (Fr) $= \bar{U}_z/\sqrt{bg}$; Cauchy number (Ca) = $\rho{\bar{U}_z}^2/GJ$. For correct similarity in behaviour between the model (m) and the prototype (p), these non-dimensional groups should be numerically equal. All these requirements could not be satisfied completely so an assessment of the relative importance of the various forces should be made. Hence, scaling of the less significant forces may be neglected. It may also be necessary to relax some of the criteria to allow a practicable model to be constructed. For instance, full-scale Re cannot be achieved in the wind tunnel. Exact maintenance of this ratio is only required when the viscous forces become of the same order of magnitude as the inertia forces. In this case, for typical Re, the flow field and pressure distributions are independent of Re and so errors due to incorrect scaling are very small. The derivation of time or velocity scales is achieved by making equal St in the model and in the full-scale structure, hence: $\left(\frac{nL}{\bar{U}}\right)_m = \left(\frac{nL}{\bar{U}}\right)_p \therefore \bar{U}_r = n_r L_r$. So, as $\bar{U}_r = L_r/T_r$, then $T_r = L_r/\bar{U}_r$. Following, if gravity forces are present, the time scale is constrained by the Fr requirement, $\left(\bar{U}/\sqrt{Lg}\right)_m = \left(\bar{U}/\sqrt{Lg}\right)_p \therefore \bar{U}_r = \sqrt{L_r g_r}$, and given that $g_r = 1$, then $\bar{U}_r = \sqrt{L_r}$, and $T_r = \sqrt{L_r}$. For any structure where the mode of resistance is torsion, Ca criterion can be modified as:

$$\left(\frac{\rho\bar{U}^2}{GJ/L^4}\right)_m = \left(\frac{\rho\bar{U}^2}{GJ/L^4}\right)_p \tag{2}$$

Where GJ is the sectional torsional rigidity. Then as the density of the air is the same for both the model and the full-scale structure, $(GJ)_r = {L_r}^4{\bar{U}_r}^2 = {L_r}^5$. The mass distribution can be approximated considering the air density ratio is 1, and by keeping constant the inertia forces ratio so that $\rho_{s_r} = 1$. Then, if mass per unit length is considered, $m_r = {L_r}^2$. The damping also needs to be modelled. For solar trackers arrays, damping is defined in the order of 3% to 15% (Rohr et al, 2015). The adjustment of the damping ratio is challenging to control in aeroelastic models.

3.2.1 Single array tests

The aim of this test is to determine loading and dynamic response of a solar tracker for a range of tilt angles (α) and wind directions (θ). Figure 2 shows a conceptual design of the single array model. Dimensions of the model can be determined using Equation 2, with an adequate length ratio (e.g. 1/200), typical materials of STS and appropriate materials for the model. Then, torque M_t on the fixed end of the torque tube and rotational displacement on the solar panels will be

measured. The array will be initially set at a defined tilt angle α. Wind speed will be increased progressively until the onset of torsional galloping, defining U_{cr} for each case. Torque will be measured with load cells attached to the fixed end. Rotational displacement γ of the plate will be video recorded with cameras oriented towards highlighted dots on the solar and then processed with a photogrammetry software.

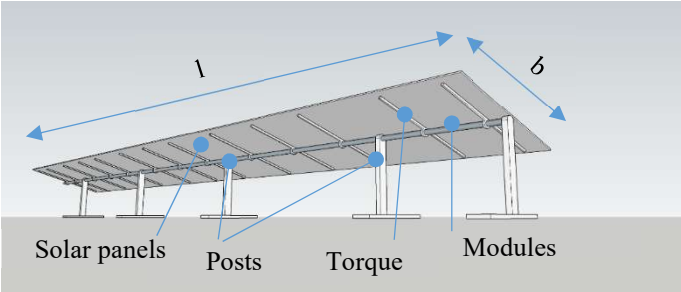

Figure 2. Single array aeroelastic model diagram

This model is replicated to create a configuration of multiple arrays. The aim in this experiment is to obtain information on how the configuration influences dynamic behaviour and to determine vibrations caused by vortex shedding. The test will consist of varying spacing between rows as well as the initial tilt angle of each array and observing how each row responds for different wind directions.

3.2.2 Sectional model test

A scaled section of an array will be built and tested in the wind tunnel to obtain detail of the aerodynamic mechanism of the plate. Typical length ratios used for such models are 1/8 to 1/10 (Taylor and Brown, 2020). Taking advantage of this scale, pressure taps may be introduced in the plate, so that pressure fluctuations can be measured. Additionally, rotational displacement and torque will be measured.

4. CONCLUSION

Wind loading on solar panels were obtained using rigid model tests. A methodology to measure forces, displacements and variables that cause dynamic instabilities is proposed to evaluate torsional galloping and vortex-induced vibrations on STS, using aeroelastic models.

REFERENCES

Blevins, R. D. (1990). Vibration of structures induced by fluid flow. McGraw-Hill handbooks, (part I).

Chen, Y., and Fang, C. (1996). "Strouhal numbers of inclined flat plates." Journal of Wind Engineering & Industrial Aerodynamics 61.

Ginger, J. D., Bodhinayake, G. G., and Ingham, S. (2019). "Wind loads for designing ground-mounted solar-panel arrays." Australian Journal of Structural Engineering 20(3): 204-218.

Martínez-García, E., Blanco-Marigorta, E., Parrondo Gayo, J., and Navarro-Manso, A. (2021). "Influence of inertia and aspect ratio on the torsional galloping of single-axis solar trackers." Engineering Structures 243.

Rohr, C., Bourke, P. A., and Banks, D. (2015). Torsional Instability of Single Axis Solar Tracking Systems. 14th International Conference on Wind Engineering. Porto Alegre - Brazil.

Taylor Z.J., and Brown M.T.L. (2020). "Hybrid pressure integration and buffeting analysis for multi-row wind loading in an array of single-axis trackers." Journal of Wind Engineering & Industrial Aerodynamics 197.

Valentín, D., Valero, C., Egusquiza, M., and Presas, A. (2022). "Failure investigation of a solar tracker due to wind-induced torsional galloping." Engineering Failure Analysis 135.